symmetry

IMPACT FACTOR 2.7

CITESCORE 4.9

Article

An Overview of the Searches for the Violation of the Charge-Parity Symmetry in the Leptonic Sector

Vyacheslav Galymov

Special Issue

Experimental Tests of Fundamental Symmetries in Particle Physics

Edited by

Dr. Giulia Brunetti and Dr. Marta Torti

MDPI

https://doi.org/10.3390/sym16010130

symmetry

MDPI

Article

An Overview of the Searches for the Violation of the Charge-Parity Symmetry in the Leptonic Sector

Vyacheslav Galymov

Institute of Physics of the 2 Infinities of Lyon, 69100 Villeurbanne, France; vgalymov@ipnl.in2p3.fr

Abstract: The existence of a violation of the Charge-Parity (CP) symmetry in the laws of physics is one of the cornerstone conditions for the generation of a matter–antimatter imbalance necessary to the creation of a matter-dominated universe. The first experimental evidence of the fact that this symmetry is broken in nature was obtained in 1964 in the observations of the decays of neutral kaon mesons. The magnitude of CP violation in the quark sector was measured with an increasing precision exploring also decays of other mesons. However, CP violation in the quark sector alone is not sufficient to explain the formation of matter-dominated universe, and additional sources are required. One such potential source is the lepton sector, where the CP violation could be observed by studying neutrino oscillations with neutrino beams generated by particle accelerators. This article reviews the present efforts in this direction. The results obtained in the ongoing experiments, T2K in Japan and NOvA in USA, are discussed. Additionally, the search for leptonic CP violation is one of the key goals in the programs of future experiments, DUNE in USA and Hyper-Kamiokande in Japan. These experiments and their prospects for its discovery are also presented.

Keywords: neutrino oscillations; long-baseline experiments; leptonic CP violation

Citation: Galymov, V. An Overview of the Searches for the Violation of the Charge-Parity Symmetry in the Leptonic Sector. *Symmetry* **2024**, *16*, 130. https://doi.org/10.3390/sym16010130

Academic Editors: Giulia Brunetti and Marta Torti

Received: 15 December 2023
Revised: 10 January 2024
Accepted: 16 January 2024
Published: 22 January 2024

1. Introduction

The visible universe (e.g., stars, galaxies) appears to be composed of the ordinary matter just like everything one encounters on Earth or in the solar system, i.e., atomic nuclei made from protons and neutrons (both belonging to the class of particles called baryons) orbited by electrons. There is no evidence for the existence of localized pockets in the universe containing only antimatter, and asymmetry between matter and antimatter appears to be close to 100%. In the framework of the Big Bang genesis, the universe expands from a superdense high-temperature initial state. In these conditions, any existence of localized distinct clusters of matter and antimatter is unlikely. Rather, particles and antiparticles co-exist in an equilibrium where their numbers are replenished continuously via the creation processes and reduced when they annihilate each other in pairs.

Following the Big Bang, the temperature of the rapidly expanding universe was quickly decreasing. Eventually, the energy needed for the creation processes became too low and annihilation took over. Annihilation continued until the particles and antiparticles became sufficiently separated from each other to interact. At this point, the number densities of baryon n_B and antibaryon $n_{\bar{B}}$ were essentially fixed. However, in the absence of any asymmetry in the laws of nature governing the interactions of particles and antiparticles, these numbers would be catastrophically low. Normalized to the photon number density n_γ, they come to [1]

$$\frac{n_B}{n_\gamma} \simeq \frac{n_{\bar{B}}}{n_\gamma} \simeq 10^{-18}.$$

This is about 10^{-9} times smaller than the value of baryonic density obtained from the measurements of the abundances of the light elements or inferred from cosmic microwave background measurements [2]:

$$\frac{n_B}{n_\gamma} \simeq 6 \times 10^{-10}.$$

Such annihilation catastrophe, where all the matter practically disappears, was evidently avoided. Starting from the symmetric state, without any excess of baryon over antibaryons, a tiny number of baryons survived and seeded the formation of planets, stars, galaxies, etc.—the baryon-dominated Universe. The three necessary conditions that any theory of the baryon creation, or baryogenesis, must fulfill in order that the Baryon Asymmetry of Universe (BAU)—the excess of baryons over antibaryons—could develop was formulated by A. Sakharov in 1967 [3]. They are

1. existence of baryon number violation,
2. existence of Charge (C) and Charge-Parity (CP) symmetry violations,
3. departure from thermal equilibrium.

The baryon number violation is evidently required to arrive to net baryon excess. Violation of C and CP is also needed to assure that reactions for particles and antiparticles have different rates. Formally, CP transformation converts a particle to an antiparticle, and a theory that is symmetric under CP does not distinguish between the two. If CP is conserved during baryogenesis, every reaction that produces a particle has a counterpart that produces its antiparticle happening at exactly the same rate, thus leading to no net baryon number in the end. As the masses of particles and antiparticles are equal, their concentrations remain forever the same in the thermal equilibrium since energetically there is no preference for the production of one or the other, hence the need for third conditions.

The remainder of this review focuses on CP violation and in particular how it can be observed in long-baseline (LBL) neutrino oscillation experiments with conventionally produced neutrino (or antineutrino) beams at particle accelerators. Typically, such experiments use two detectors, one located near the beam origin (near detector) and the other placed far away (far detector), in order to assess the neutrino beam original characteristics (e.g., energy spectrum and flavor content) and measure its composition after significant flavor oscillations, respectively. A precise analysis of the oscillations of neutrinos in comparison to antineutrinos could then allow determining whether CP symmetry is preserved. The existence of CP violation in the lepton sector is one of the cornerstones of leptogenesis, a framework within which one tries to generate an asymmetry between lepton and antilepton numbers and to convert it into BAU.

2. Quark Mixing and CP Violation

The existence of a CP violation in the quark sector was first observed in 1964 in the decay properties of neutral kaons [4]. Within the Standard Model (SM) of particle physics, CP violation is embedded in the Cabibbo–Kobayashi–Maskawa (CKM) mixing matrix, V_{CKM}, which relates that quark mass states participate in the flavor-changing weak interactions mediated by $W^{\pm}$ boson exchange (charge current interactions). This 3×3 unitary matrix ($V^{\dagger}V = 1$),

$$V_{\mathrm{CKM}} = \begin{pmatrix} V_{ud} & V_{us} & V_{ub} \\ V_{cd} & V_{cs} & V_{cb} \\ V_{td} & V_{ts} & V_{tb} \end{pmatrix}, \tag{1}$$

physically describes the linear combination of left-handed components of down-type quarks d, s, b that participate in the charged current reactions with up-type quarks u, c, t.

The CKM matrix can be parameterized in terms of three mixing angles θ_{12}, θ_{23}, θ_{13}, and a complex phase δ_{CP} [2]:

$$V_{\mathrm{CKM}} = \begin{pmatrix} c_{12}c_{13} & s_{12}c_{13} & s_{13}e^{-i\delta_{CP}} \\ -s_{12}c_{23} - c_{12}s_{23}s_{13}e^{i\delta_{CP}} & c_{12}c_{23} - s_{12}s_{23}s_{13}e^{i\delta_{CP}} & s_{23}c_{13} \\ s_{12}s_{23} - c_{12}c_{23}s_{13}e^{i\delta_{CP}} & -c_{12}s_{23} - s_{12}c_{23}s_{13}e^{i\delta_{CP}} & c_{23}c_{13} \end{pmatrix}, \tag{2}$$

where s_{ij} and c_{ij} are the short-hands for $\sin\theta_{ij}$ and $\cos\theta_{ij}$, respectively.

While non-vanishing δ_{CP} implies the violation of CP in the standard model, this phase in itself, however, is not a good measure. It is dependent on a particular choice of parametrization and could be shifted to different elements of the matrix by rephasing the fields. A parametrization-invariant measure of the CP violation can, however, be constructed from four products of CKM elements, $V_{\alpha j}V_{\beta i}V^*_{\alpha i}V^*_{\beta j}$ ($\alpha \neq \beta$ and $i \neq j$). For CP violation to occur, V_{CKM} must be complex and the imaginary part of these products non-vanishing. Moreover, $\Im\mathfrak{m}(V_{\alpha j}V_{\beta i}V^*_{\alpha i}V^*_{\beta j})$ are all equal up to a sign to a constant called Jarlskog invariant [5]. Without the loss of generality, one can define it to be given by

$$J_{CP} = \Im\mathfrak{m}(V_{us}V_{cb}V^*_{ub}V^*_{cs}), \tag{3}$$

and with parametrization of Equation (2), it can be expressed as

$$J_{CP} = c_{12}s_{12}c_{23}s_{23}c^2_{13}s_{13}\sin\delta_{CP} \equiv J^{max}_{CP}\sin\delta_{CP}, \tag{4}$$

with

$$J^{max}_{CP} \equiv c_{12}s_{12}c_{23}s_{23}c^2_{13}s_{13} \tag{5}$$

representing the maximum possible magnitude of the invariant when $|\sin\delta_{CP}| = 1$.

The components of the CKM matrix have been extensively measured to a high precision from a variety of meson states. The values of the sines of the mixing angles currently are [2]

$$s_{12} = 0.22500 \pm 0.00067, \qquad s_{23} = 0.04182^{+0.00085}_{-0.00074}, \qquad s_{13} = 0.00369 \pm 0.00011. \tag{6}$$

The value of a complex CKM CP phase is [2]

$$\delta^{(\mathrm{CKM})}_{CP} = 1.144 \pm 0.027 \sim 66^\circ, \tag{7}$$

and that of the CKM Jarlskog invariant is [2]

$$J^{(\mathrm{CKM})}_{CP} = (3.08^{+0.15}_{-0.13}) \times 10^{-5}. \tag{8}$$

However, this (extremely well-measured) CP violation contained in the CKM matrix alone appears to be by far insufficient for BAU generation (e.g., [1,6]). It leads to a conjecture that there must be other sources of CP violation in nature, and significant experimental efforts are being dedicated to searching for any deviations from SM description within the quark sector. On the other hand, the evidence of the neutrinos having a non-zero mass, as a consequence to the observations of the neutrino oscillations, opened up an additional avenue to explore CP violation in the lepton sector.

3. Neutrino Mixing and CP Violation

Neutrino mixing arises from the fact that flavor neutrino states ν_e, ν_μ, and ν_τ which take part in the weak charged current reactions with their charged counterparts e, μ, τ are not the proper mass states, but a linear combination of such. Similar to quarks, the mixing is described by a unitary 3×3 matrix U named after Pontecorvo, Maki, Nakagawa, and Sakahata (PMNS):

$$U_{\mathrm{PMNS}} = \begin{pmatrix} U_{e1} & U_{e2} & U_{e3} \\ U_{\mu 1} & U_{\mu 2} & U_{\mu 3} \\ U_{\tau 1} & U_{\tau 2} & U_{\tau 3} \end{pmatrix}. \tag{9}$$

The elements of U_{PMNS}, as for V_{CKM}, can be parameterized in terms of three mixing angles θ_{12}, θ_{23}, θ_{13} and complex phase δ_{CP} yielding the same form as Equation (2). However, since neutrinos are electrically neutral, they could potentially also be their own antiparticles: so-called Majorana fermions, as opposed to Dirac fermions, such as quarks and charged

leptons. In that case, the mixing matrix contains two additional CP violating phases α_1 and α_2:

$$U_{\mathrm{PMNS}}^{(M)} = UM, \qquad M = \mathrm{diag}(e^{i\alpha_1}, e^{i\alpha_2}, 1), \tag{10}$$

where matrix U has the same elements as Equation (2). The LBL neutrino oscillation experiments have no sensitivity to the two *Majorana* phases as they do not enter into the oscillation probabilities that one can measure. However, some possibility exists to probe their values [7] if searches for the neutrinoless double beta decay process are successful and neutrinos are indeed Majorana particles.

Neutrino mixing angles show a strikingly different pattern from that of quarks. Based on the values from a global fit to experimental data [8,9], the sines of the PMNS mixing angles are

$$s_{12} = 0.55 \pm 0.009, \qquad s_{23} = 0.756 \pm 0.013, \qquad s_{13} = 0.148 \pm 0.002. \tag{11}$$

Comparing them to those of CKM (Equation (6)), one can see that, in the case of neutrino mixing, s_{23} and in particular s_{13} are rather large. Consequently, if leptonic CP violation is at or near maximal, $|\sin\delta_{CP}| \approx 1$, the value of the Jarlskog invariant is close to J_{CP}^{max} and, with the latter currently at [2]

$$J_{CP}^{max} = (3.359 \pm 0.06) \times 10^{-2}, \tag{12}$$

the CP violation in the lepton sector could potentially be larger than that in the quark sector (Equation (8)) by up to three orders of magnitude.

Apart from possibly hiding the source of a large CP violation, what also sets neutrinos apart from other SM elementary particles (quarks and charged leptons) is the extreme smallness of their masses. The scale of the neutrino mass could be probed via precise measurements of the endpoint of the energy spectrum of electrons emitted in β decays of tritium. The most stringent limit on the neutrino mass using this approach was set by the KATRIN experiment in 2022 [10]:

$$m_\nu < 0.8\,\mathrm{eV} \text{ at } 90\% \text{ confidence level.}$$

The mass scale can also be constraints from cosmological data. For example, the Planck measurements of the cosmic microwave background set the upper limit on the neutrino masses at 0.12 eV [11]. At this level, neutrinos appear to be lighter than electron—itself the lightest of the charged elementary particles—by a factor of almost 10^6.

In the standard model, the particle masses are generated via the interaction with the Higgs boson that couples chirally left-handed fermion fields to right-handed ones. As the right-handed neutrinos have never been observed, within the standard model, neutrinos were naturally considered to be massless. However, the observations of the neutrino oscillations proved otherwise.

Given the smallness of the neutrino mass scale, it appears to be unlikely their masses can be generated by the same mechanism as other fermions. The most popular scenario for the explanation of light neutrino masses is a See-Saw mechanism [12] that relies on the fact that neutrinos could be Majorana particles and associates an exceptionally heavy right-handed neutral (Majorana) partner N to the light neutrino. In this model, as the name suggests, the lighter the ν, the heavier the N must be. With its mass somewhere in the range of 10^{12} GeV to 10^{15} GeV, N cannot be created in particle accelerators. On the other hand, such particles could be produced after the Big Bang when the temperature of the early universe was still very high and their numbers were effectively frozen once the temperature decreased. N could then decay both to charged leptons and antileptons. However, if leptonic CP violation exists, these decays would not have the same rates, leading eventually to an asymmetry between the number of leptons and antileptons that, in turn, could be converted into baryon–antibaryon asymmetry.

This procedure for generating BAU from an imbalance in lepton–antilepton numbers as a result of the decays of a heavy neutral particle is leptogenesis [13]. While one cannot probe directly the existence of N, we could hope to discover some supporting clues such as whether neutrinos are Majorana fermions and whether the CP symmetry is broken in the leptonic sector.

4. Neutrino Oscillations

Neutrino mixing gives rise to the phenomenon of neutrino oscillations whereby a beam of neutrinos of a given flavor α ($\alpha = e, \mu, \tau$) periodically changes its composition by exhibiting presence of other flavors β as it propagates through space. In this context, the neutrino flavor is defined based on the type of the charged lepton that is produced (and detected) in charged current reactions.

The probability for neutrinos remaining in initial state α (survival) or oscillating to another flavor β (appearance) is determined by the elements of the PMNS mixing matrix and the differences between neutrino mass squares $\Delta m^2_{ij} \equiv m^2_i - m^2_j$ ($i, j = 1, 2, 3$). For the case of three active neutrinos (antineutrinos), it can be written compactly:

$$\begin{array}{c} P_{\nu_\alpha \to \nu_\beta}(P_{\bar{\nu}_\alpha \to \bar{\nu}_\beta}) = \delta_{\alpha\beta} - 4\sum_{i>j} \mathfrak{Re}(U^*_{\alpha i} U_{\beta i} U_{\alpha j} U^*_{\beta j}) \sin^2 \Delta_{ij} \\ \pm 2\sum_{i>j} \mathfrak{Im}(U^*_{\alpha i} U_{\beta i} U_{\alpha j} U^*_{\beta j}) \sin 2\Delta_{ij}, \end{array} \tag{13}$$

where

$$\Delta_{ij} \equiv \frac{\Delta m^2_{ij} L}{4E} = 1.267 \Delta m^2_{ij}(\mathrm{eV}^2) \frac{L(\mathrm{km})}{E(\mathrm{GeV})} \tag{14}$$

and $\delta_{\alpha\beta}$ is the Kronercker delta, E is the neutrino energy, and L is the distance from a neutrino source to a detector (baseline of an experiment). The plus (minus) in front of the last term in Equation (13) is for neutrinos (antineutrinos). For three neutrino mass states with masses m_1, m_2, and m_3, there are only two independent Δm^2_{ij}. The smaller of the two Δm^2_{21} has the value of about $7.4 \times 10^{-5}\,\mathrm{eV}^2$ and historically has been associated with the measurements of solar neutrino fluxes. The other could be taken to be Δm^2_{31} or Δm^2_{32} and has a much larger value of around $2.5 \times 10^{-3}\,\mathrm{eV}^2$. It was initially measured in the oscillation of atmospheric neutrinos propagating through Earth. While the sign of Δm^2_{21} is known, i.e., one can say that the state with mass m_1 is lighter than the one with m_2, this is not the case for Δm^2_{31} for which only the absolute value is currently determined. Thus, two configurations for the hierarchy or ordering of neutrino masses are possible: one where the state with m_3 is the heaviest and the other where it is the lightest. Traditionally, the former is referred to as Normal Ordering (NO), while the latter is called Inverted Ordering (IO).

The four products, $U^*_{\alpha j} U_{\beta j} U_{\alpha i} U^*_{\beta i}$, in Equation (13) for the survival probability ($\alpha = \beta$) are real, and therefore CP violation can be detected only through appearance channels ($\alpha \neq \beta$). The imaginary part of any non-zero four-product is equal to the invariant J_{CP} from Equation (4) up to a sign. Introducing asymmetry factor

$$A_{\alpha\beta} = P_{\nu_\alpha \to \nu_\beta} - P_{\bar{\nu}_\alpha \to \bar{\nu}_\beta}, \tag{15}$$

one can trivially see that CP symmetry is preserved when $A_{\alpha\beta} = 0$.

The LBL experiments so far, as well as the ones in the immediate future, rely on conventional neutrino beams [14] where the neutrinos are produced mainly in the decays of $\pi^\pm$ mesons generated in high-energy collisions of a primary accelerated proton beam with a stationary target. The charge selection of the pions is performed by a system of focusing elements (magnetic horns) allowing production of beams of mostly pure ν_μ or $\bar{\nu}_\mu$. For CP measurement with such beams, the principal channel is $\nu_\mu \to \nu_e$ appearance. The asymmetry factor of interest is then $A_{\mu e}$, which can be written as

$$A_{\mu e} = -16 J_{CP} \sin \Delta_{21} \sin \Delta_{32} \sin \Delta_{31}. \tag{16}$$

For CP violation to be observed, not only the invariant J_{CP} must be non-zero, but also the three neutrino masses must be distinct. The LBL experiments so far have been tuned to sample the oscillation probability at first maximum driven by $\sim \Delta m^2_{31}$, that is to say when $\sin\Delta_{32} \simeq \sin\Delta_{31} \approx 1$. From Equation (14), this condition is fulfilled when

$$\frac{L}{E} = \frac{\pi}{1.267\Delta m^2_{31}}(n + 1/2),\ n = 0, 1, 2..., \tag{17}$$

where $n = 0$ is the first oscillation maximum, $n = 1$ is the second, etc. Taking L/E at the first maximum, the value that the asymmetry in Equation (16) can attain there is

$$\mathrm{Max}(A_{\mu e}) \approx -16 J_{CP} \sin\left(\frac{\Delta m^2_{21}}{\Delta m^2_{31}}\frac{\pi}{2}\right), \tag{18}$$

which is about ± 0.025 when $\sin\delta_{CP} = \mp 1$.

The asymmetry expressed by Equation (16) is only valid for the neutrinos propagating in a vacuum. In reality, the neutrino beams travel through Earth along the chords that penetrate the crust at varying depths. The neutrinos can then undergo coherent scattering from in the atomic electrons in the surrounding medium, which introduces additional phases in the oscillation amplitudes that are different for neutrinos and antineutrinos. The effect of the matter is included in oscillation probability calculations via introduction of effective matter potential V, which is proportional to the number density of electrons n_e in the encountered medium:

$$V = \sqrt{2} G_F n_e, \tag{19}$$

where G_F is the Fermi constant.

Assuming a uniform average electron density, that is to say, constant along the beam path, the oscillation probability for the $\nu_\mu \to \nu_e$ appearance channel can be approximated by [15]

$$P_{\nu_\mu \to \nu_e} \approx \sin^2 2\theta_{13} \sin^2\theta_{23} \frac{\sin^2\left((1-A)\Delta_{31}\right)}{(1-A)^2} + \alpha^2 \sin^2 2\theta_{12} \cos^2\theta_{23} \frac{\sin^2\left(A\Delta_{31}\right)}{A^2} + \alpha 8 J^{\max}_{CP} \cos(\Delta_{31} + \delta_{CP}) \frac{\sin\left(A\Delta_{31}\right)}{A} \frac{\sin\left((1-A)\Delta_{31}\right)}{(1-A)}, \tag{20}$$

where J^{max}_{CP} and Δ_{ij} are defined in Equations (5) and (14), respectively, while

$$A \equiv \frac{2VE_\nu}{\Delta m^2_{31}}, \tag{21}$$

$$\alpha \equiv \frac{\Delta m^2_{21}}{\Delta m^2_{31}}. \tag{22}$$

For the equivalent antineutrino channel, one must flip the signs of the CP phase and the effective matter potential: $\delta_{CP} \to -\delta_{CP}$ and $V \to -V$.

The first term in Equation (20) is the leading contribution to the oscillation probability for this channel that allowed the measuring of the θ_{13} mixing angle in LBL experiments [16,17]. Given the sizes of Δm^2_{21} and Δm^2_{31}, the second term has a negligible contribution to the oscillation probability as $\alpha^2 \simeq 0.0009$. The last term introduces sub-leading effects dependent on the value of the δ_{CP} phase, which one then must measure. Additionally, since the matter effects introduce a phase to the oscillations driven by Δm^2_{31}, the ordering of the neutrino masses could also be determined.

The matter effect generates an asymmetry for neutrino and antineutrino oscillations and its impact grows with the distance the neutrino beam travels (i.e., amount of material it encounters) and neutrino beam energy. The electron number density in Equation (19) is proportional to the matter density as $n_e \simeq 0.5 N_A \rho \mathrm{cm}^{-3}$, where the factor of 0.5 is an

approximate value for the ratio of electron to nucleon number densities for ordinary matter and N_A is the Avogadro number. Dimensionally, the numerator of Equation (21) must have the same units as Δm^2_{31} and, with the latter measured in eV^2, one obtains

$$2VE_\nu \simeq 7.6 \times 10^{-5} \rho(\mathrm{g/cm^3}) E_\nu(\mathrm{GeV}) \mathrm{eV}^2. \tag{23}$$

Equations (23) and (21) show the proportionality of matter-induced phase A to neutrino energy. Alternatively, Equation (20) can be recast to make the dependence on baseline length L explicit by expanding $A\Delta_{31}$ products. Following [18], one can define distance scale parameter a,

$$a = \pm \frac{G_F n_e}{\sqrt{2}}, \tag{24}$$

with a positive (negative) sign for neutrinos (antineutrinos). Then, with

$$A\Delta_{31} = \frac{G_F n_e}{\sqrt{2}} L = aL, \tag{25}$$

the oscillation probability of Equation (20) can be rewritten as

$$P_{\nu_\mu \to \nu_e} \approx \sin^2 2\theta_{13} \sin^2 \theta_{23} \frac{\sin^2(\Delta_{31} - aL)}{(\Delta_{31} - aL)^2} \Delta^2_{31} + \sin^2 2\theta_{12} \cos^2 \theta_{23} \frac{\sin^2(aL)}{(aL)^2} \Delta^2_{21} + 8 J^{\max}_{CP} \cos(\Delta_{31} + \delta_{CP}) \frac{\sin(aL)}{(aL)} \frac{\sin(\Delta_{31} - aL)}{(\Delta_{31} - aL)} \Delta_{31} \Delta_{21}. \tag{26}$$

With L typically being in km, the units of a must be cast to km^{-1}. Switching from natural units by re-introducing $\hbar$ and c factors one finds

$$a \simeq 9.629 \times 10^{-5} \rho(\mathrm{g/cm^3}) \mathrm{km}^{-1}. \tag{27}$$

As an example, taking a matter density of 2.8 g cm^{-3} (an approximate value if the beam travels through the upper crust layer of the Earth), one obtains $a \sim 1/3700$ km^{-1} as a measure of a distance scale.

The current and the next-generation LBL neutrino oscillation experiments have baseline lengths ranging from about 300 km to 1300 km. Figure 1 attempts to illustrate qualitatively the evolution of the impact of the matter effect on the ν_e appearance probability as a function of L. The vertical axis in the figure shows a mean asymmetry factor, $< A_{\mu e} >_{\mathrm{FWHM}}$, computed from the averaged oscillation probabilities for neutrinos and antineutrinos over an energy window defined by a full width at half maximum of the first oscillation peak:

$$< A_{\mu e} >_{\mathrm{FWHM}} = < P_{\nu_\mu \to \nu_e} >_{\mathrm{FWHM}} - < P_{\bar{\nu}_\mu \to \bar{\nu}_e} >_{\mathrm{FWHM}} . \tag{28}$$

This is rather a simplification, as typically one does not perform a single measurement but attempts to fit the shape of the probability by sampling around its maximum value in an energy window defined by the beam energy spectrum, event reconstruction efficiencies and selection cuts, etc. However, the plot still serves as a convenient illustration for a number of features.

Each band in Figure 1 represents the different possible values of $< A_{\mu e} >_{\mathrm{FWHM}}$ depending on the value of the δ_{CP} phase for a given mass ordering as a function of baseline length. Some representative cases for the choices of δ_{CP} like the CP-conserving values $\delta_{CP} = 0, \pi$ or those with $\delta_{CP} = \pm\pi/2$ corresponding to the maximal CP violation are also superimposed. Without the knowledge of mass ordering, the experiments with shorter baselines (where the two bands overlap) lose sensitivity to parts of the δ_{CP} parameter space due to a degeneracy introduced by the two unknowns, δ_{CP} and sign of Δm^2_{31}. In particular, one could even obtain similar asymmetry generated by CP-conserving phase

values, $\delta_{CP} = 0, \pi$, in one mass ordering scenario as that produced by phases $\pm\pi/2$ (i.e., the phase values corresponding to the maximal CP violation) for the other mass ordering. In Figure 1, such cases correspond to the points where edges of a given band intersect the $\delta_{CP} = 0, \pi$ lines in the other band. Without the knowledge of mass ordering, one could incorrectly infer the existence or non-existence of CP violation.

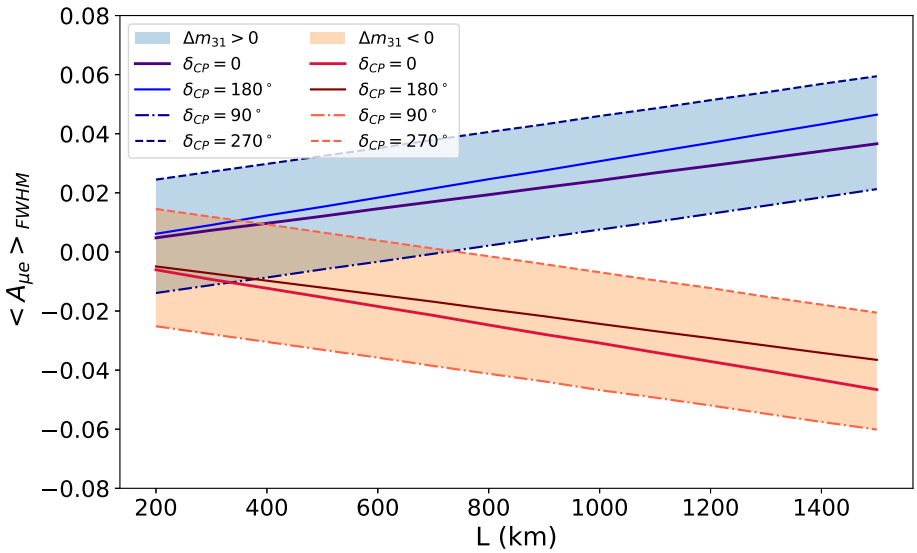

Figure 1. Asymmetry averaged over an energy window given by the full width at half maximum of ν_e ($\bar{\nu}_e$) appearance probabilities, computed with Equation (26), as a function of the baseline. A constant density of 2.8 g cm^{-3} is assumed and the values of other oscillation parameters (θ_{ij} and Δm^2_{ij}), apart from δ_{CP}, are taken from [8,9]. Asymmetry is shown for the two possible neutrino mass orderings with the bands indicating variation from different possible δ_{CP} values.

As the effect of matter grows with baseline length, acquired phase aL in Equation (26) causes increasing enhancement (suppression) or suppression (enhancement) of appearance probability for neutrinos (antineutrinos) depending on the underlying ordering of neutrino masses. The two bands in Figure 1 begin to separate at about 800 km until eventually they are so far apart that one can readily distinguish the two possible mass ordering scenarios and measure δ_{CP} at the same time. The matter effect could also lead to breaking the degeneracy between the two CP-conserving $0, \pi$ phase values as illustrated by an increasing separation of the two corresponding lines for each choice of mass ordering.

For further illustration, ν_e and $\bar{\nu}_e$ appearance probabilities at the first oscillation maximum for a 1300 km baseline are also plotted in Figure 2 for the CP conserving case and the maximal CP violation as well as both mass orderings. The enhancement or suppression, depending on the sign of Δm^2_{31}, of ν_e or $\bar{\nu}_e$ appearance can be clearly seen.

One could notice from Equation (26) that the second and third (Δ^2_{21} and CP phase-sensitive) terms disappear when product aL is a multiple of π. The first such "magic" baseline is

$$L_{\mathrm{m}} = \frac{\pi}{a} = \frac{\sqrt{2}}{G_F n_e}\pi \tag{29}$$

and, depending on assumed density profile, its value can be $L_{\mathrm{m}} \sim 7000$ km to 8000 km. Experiments searching for neutrino electron appearance on magic baselines were suggested early on to help disentangle contributions from multiple unknowns (θ_{13}, δ_{CP}, sign of Δm^2_{31}) to the oscillation probability for this channel.

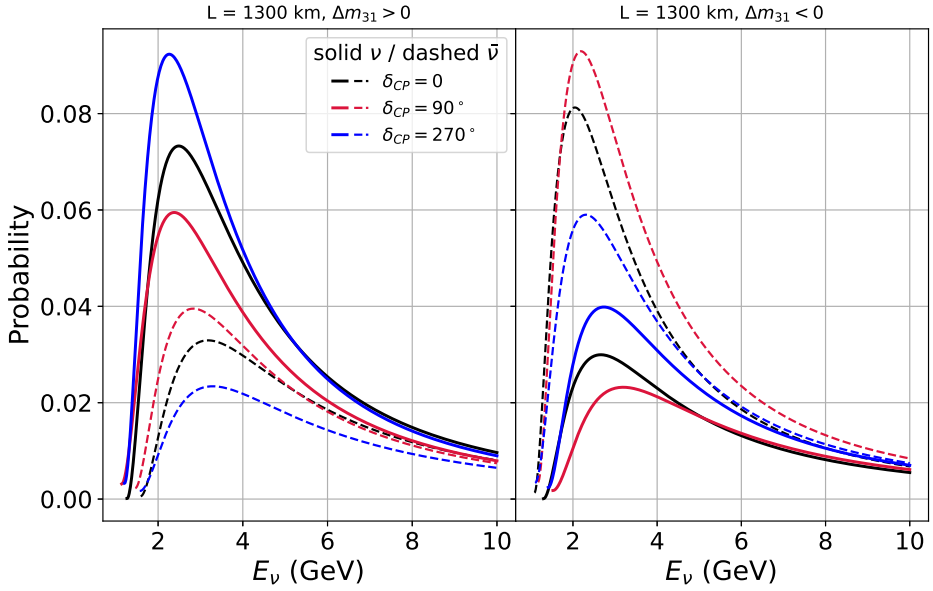

Figure 2. The first maximum of $\nu_\mu \to \nu_e$ ($\bar{\nu}_\mu \to \bar{\nu}_e$) appearance probability shown in solid (dashed) curves for a set of values of δ_{CP} as a function of (anti)neutrino energy for a baseline of 1300 km computed with Equation (26). The panel on the left (right) is for normal (inverted) neutrino mass ordering. A constant density of 2.8 g cm^{-3} is assumed, and the values of other oscillation parameters (θ_{ij} and Δm^2_{ij}), apart from δ_{CP}, are taken from [8,9].

5. Experimental Landscape

Spurred by the discovery that the value of θ_{13}, the last mixing measured angle, is rather large, the neutrino oscillation experiments are now entering the precision era focusing on the remaining unknowns such as the existence of CP violation, the ordering of neutrino masses, and determination where θ_{23} is with respect to 45° (octant). However, to offer a little historical perspective of this development, one could recall that in the first decade of this century, the knowledge of θ_{13} was limited to the exclusion region set in 2003 by the Chooz reactor experiment [19] looking at the survival of electron antineutrinos produced in nuclear reactors. The experiment was configured (the source–detector distance) to probe the oscillations driven by large $\Delta m^2_{\text{atm}} \simeq \Delta m^2_{31}$ that was also measured in a Super-Kamiokande detector from the observations of the disappearance of ν_μ component of atmospheric neutrinos [20].

When Δm^2_{31} sets dominant frequency, the reactor neutrino survival probability is approximately given by

$$P_{\bar{\nu}_e \to \bar{\nu}_e} \approx 1 - \sin^2 2\theta_{13} \sin^2 \Delta_{31}, \tag{30}$$

and this channel provides the most direct access for measuring θ_{13}. Unfortunately, with $L/E \sim 300$, Chooz was more sensitive to larger Δm^2_{31} than what it turned out to be. It saw no evidence for the disappearance of reactor antineutrinos over the baseline distance of about a kilometer excluding the values of $\sin^2 2\theta_{13}$ greater than about 0.1.

The non-zero value of θ_{13} is required for the possibility of the existence of leptonic CP violation, and a next generation of experiments, both accelerator and reactor-based ([21–23]), was then needed to look for this mixing angle. In Japan, a T2K experiment was proposed [24] to use a new high-power J-PARC accelerator for the ν_μ ($\bar{\nu}_\mu$) neutrino source with Super-Kamiokande, a 50 kt water detector, as the far detector 295 km away. Its goal was to probe $\nu_\mu \to \nu_\mu$ survival and $\nu_\mu \to \nu_e$ appearance channels at the first oscillation maximum with a neutrino beam tuned in a narrow energy window (narrow-band beam) around 0.6 GeV using the off-axis technique [25], where the far detector baseline is offset relative to the beam axis by a small angle to decrease the neutrino beam energy spread. In particular for the appearance channel, which to the first order depends on the product of

$\sin^2\theta_{23}\sin^2 2\theta_{13}$ (Equation (20)), the aim was to push the limit on $\sin^2 2\theta_{13}$ by more than one order of magnitude below 0.01.

In the USA, an accelerator-based neutrino experiment NOvA was proposed [26] with an off-axis neutrino beam originating from Fermilab and travelling 810 km to a far site equipped with a 14 kt liquid scintillator detector. Similar to T2K, one of the principal aims was to discover $\sin^2 2\theta_{13}$ also with a possibility to probe the mass ordering exploiting the larger matter effect due to the longer baseline.

As an alternative to conventional neutrino beams, the concept of muon storage rings that could be used to produce intense and easily characterized neutrino beams (neutrino factory) was pursued through a rich R&D program (e.g., [27,28]). If $\sin^2 2\theta_{13}$ turned out to be quite small, $\ll 0.1$, the neutrino factory as a source appeared as a viable solution for exploring CP violation in the lepton sector. As a substitute for stored muons, ion storage rings for β decaying isotopes producing electron (anti)neutrino beams (beta beams) were also proposed [29].

In 2011, T2K announced a first hint of a non-zero $\sin^2 2\theta_{13}$ [30]. The value itself was reported a year later by the Daya Bay reactor neutrino experiment [31] at more than 5σ significance, and it was

$$\sin^2 2\theta_{13} = 0.092 \pm 0.016(\text{stat}) \pm 0.005(\text{syst}),$$

which happened to be just below the Chooz exclusion region. Since then, it was measured with increasing precision, particularly by the reactor experiments, with the Daya Bay final result determining $\sin^2 2\theta_{13}$ to be better than 3% [32]:

$$\sin^2 2\theta_{13} = 0.0851 \pm 0.0024.$$

With such a large and tightly constrained value, the measurement of leptonic CP violation with conventionally produced neutrino beams are a distinct possibility.

In 2020, T2K reported [33] first indication of a possible existence of CP violation in the lepton sector. Their data disfavored the CP conserving values of phase $\delta_{CP} = 0, \pi$ at a 95% confidence level showing a preference for δ_{CP} for close maximal CP violation instead. Further analysis of the data collected by the experiment so far [34] put the constraint on δ_{CP} at

$$\delta_{CP} = -1.97^{+0.97}_{-0.62} = (-0.627^{+0.309}_{-0.197})\pi$$

for T2K favored solution of normal mass ordering and including the constraint on θ_{13} from reactor experiments. Figure 3 from [34] illustrates graphically the preference of the T2K data collected with the neutrino (abscissa) and antineutrino (ordinate) beam modes for the solutions that lead to the largest asymmetry in favor of ν_e ($\delta_{CP} = -\pi/2$) rather than $\bar{\nu}_e$ appearance ($\delta_{CP} = \pi/2$). The preference for $\theta_{23} > \pi/4$, which tends to simultaneously increase the expected number of events in both sets, is also visible.

While T2K appears to favor the existence of close to maximal CP violation with $\delta_{CP} \sim -\pi/2$, the results reported by the NOvA experiment do not share the same trend [35]. The analysis of the data collected up to 2020 does not exhibit strong asymmetry between electron neutrino and antineutrino appearance probabilities. Figure 4 from [34] shows the NOvA 90% confidence level contours in the $\sin^2\theta_{23}$-δ_{CP} parameter plane for each mass ordering scenario compared to T2K as well as the results from the Super-Kamiokande analysis of atmospheric neutrino sample [36]. The NOvA best fit point for δ_{CP} is close to the CP-conserving value π:

$$\delta_{CP} = (0.82^{+0.27}_{-0.87})\pi.$$

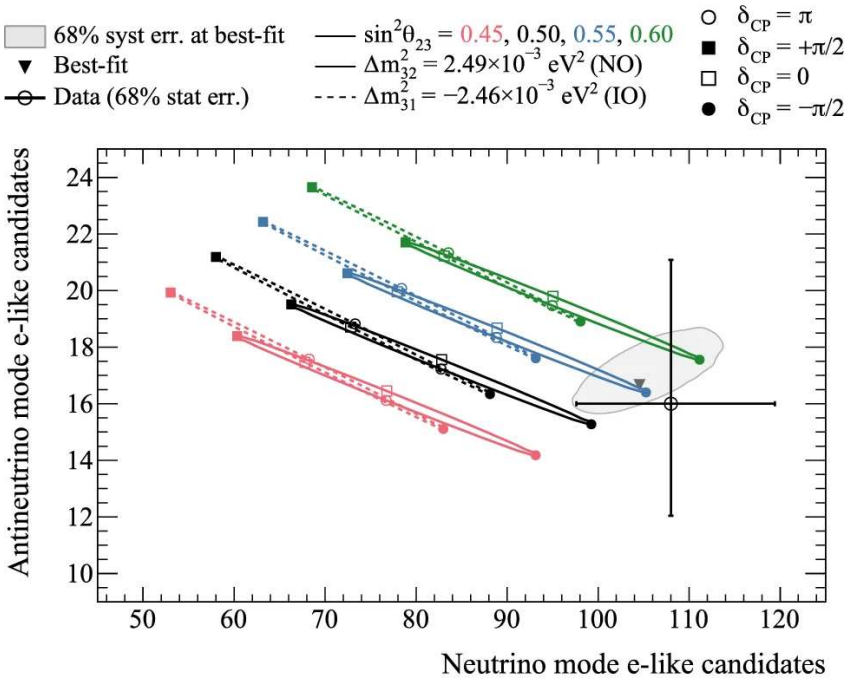

Figure 3. The number of events ν_e like events from running in ν beam versus $\bar{\nu}$ beam modes is taken from [34]. The region in grey corresponds to the best fit values of oscillation parameters based on the collected data, while the somewhat elliptical coloured contours indicate expected event numbers in each category under different hypothesis for $\sin^2\theta_{23}$, δ_{CP}, and the sign of mass ordering.

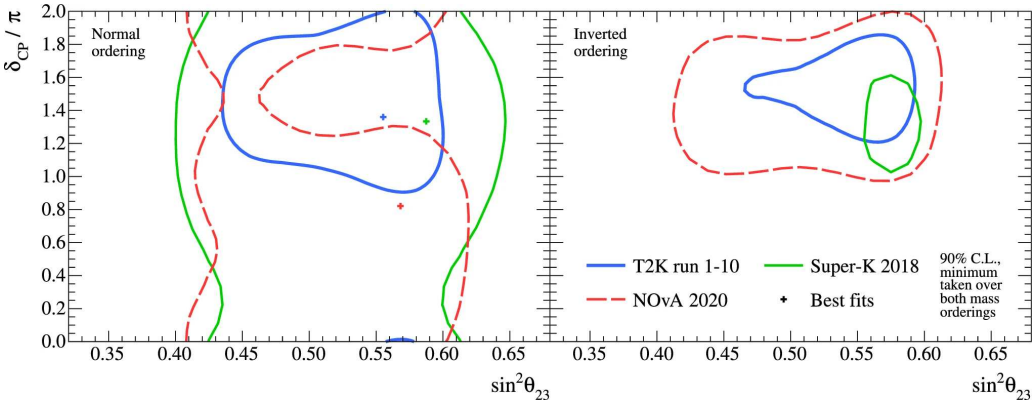

Figure 4. T2K, NOvA, and Super-Kamiokande 90% confidence level contours in the $\sin^2\theta_{23}$-δ_{CP} parameter plane for normal (**left panel**) and inverted (**right panel**) mass ordering taken from [34]. The best fit point for each experiment is denoted by a cross.

The T2K preferred solution for $\delta_{CP} \sim -\pi/2$ and NO appears to be partially disfavored by the current NOvA data, although an overlap between two results remains. In the case of IO, NOvA rules out maximal CP violation at $\delta_{CP} = \pi/2$ at more than 3σ level. On the other hand, its contours for this mass ordering scenario contain entirely the corresponding region from T2K. Although IO is disfavored both by T2K and Super-Kamiokande, in the absence of any further strong constraint on mass ordering, the solution with inverted mass ordering and CP violation close to maximal with $\delta_{CP} \sim -\pi/2$ is not ruled out. Both NOvA and T2K experiments are scheduled to continue collecting data through 2026 at least doubling statistics of their datasets. This potentially could allow mass ordering reaching 3σ sensitivity and exclude CP conservation $> 99\%$ confidence level within the next few years.

The search for leptonic CP violation is one of the key elements of the physics programs for the next generation of the LBL neutrino oscillation experiments, Hyper-Kamiokande [37] and DUNE [38], both currently in a construction stage.

The Hyper-Kamiokande detector is a water detector about five times larger than Super-Kamiokande with a total detector mass of 258 kt. The detector is located at the same off-axis angle with respect to the T2K beamline as the Super-Kamiokande as well as the same 295 km distance from J-PARC where the planned upgrades to the accelerator complex are expected to raise the beam power to 1.3 MW.

Figure 5 shows projected sensitivity of the Hyper-Kamiokande experiment as a function of a number of years of running to exclude CP conservation ($\sin\delta_{CP} = 0$). The constraint, whether from external measurements or analysis of atmospheric neutrino data sample collected Hyper-Kamiokande, on mass ordering is required in order to maximize the sensitivity of the experiment. With the knowledge of mass ordering and if CP violation is close to maximal at $\delta_{CP} \sim -\pi/2$, the value currently favored by T2K, the experiment can discover (5σ level significance) leptonic CP violation within three years of running with the start of the operation currently projected to be in 2027.

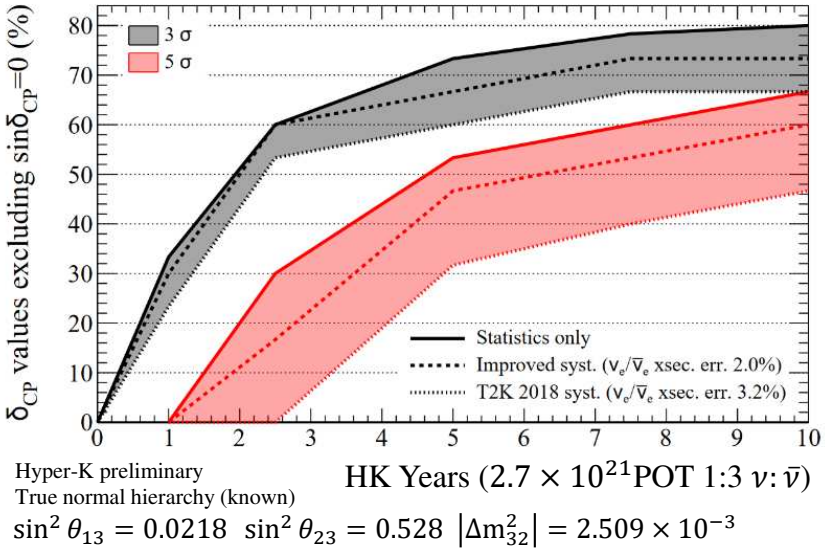

Figure 5. The fraction of δ_{CP} parameter space for which CP conservation could be excluded with 3σ (black) or 5σ confidence level from [39]. Prior knowledge of mass ordering is assumed.

The US-based DUNE experiment utilizes large liquid argon time-projected chambers as the neutrino detectors for the analysis of the neutrino beam produced at the Fermilab accelerator complex located about 1300 km away. The design foresees four modules each containing 17 kt of liquid argon. The construction is organized in phases. Within the first phase, the first two modules are scheduled to be in operation by mid-2030 [40] and the neutrino beam running in 2031. The beam power is progressively raised to 1.2 MW and further upgraded to above 2 MW as part of the second phase of the experiment also featuring an addition of two more detector modules.

Given the length of the DUNE baseline, the large matter-induced asymmetry allows for the experiment to resolve the mass ordering within few years of running in the first phase of the program independent of the δ_{CP} value. If CP violation is nearly maximal, the experiment could also potentially see it at a level of 3σ in the first phase. However, to increase the precision and enlarge the coverage of the δ_{CP} parameter space, implementation of the second phase of the project is required. This is illustrated in Figure 6, which shows the evolution of the sensitivity of DUNE to CP violation as a function of time.

Both DUNE and Hyper-Kamiokande are poised to collect a large sample of neutrino events. However, the precision measurement of CP violation also requires a tight control of systematic uncertainties for both experiments. The principal sources of the latter are related to the knowledge of the neutrino fluxes produced at the accelerators and the cross-sections for neutrino interactions. Both of these impact the rates as well as the (energy) spectra of events observable in far detectors from which one tries to infer the parameters (e.g., δ_{CP})

determining the underlying neutrino oscillation probability. Dedicated measurements of hadron production yields from different target materials help put constrains on flux uncertainties. However, a judicious design of near detectors is also required to amply characterize the properties of the neutrino beam at the production point and constraint the interaction models in the neutrino beam energy window. From this information, one then formulates the prediction for the expected observable at the far detector against which the collected data could be compared in order to extract the values of the underlying neutrino mixing parameters.

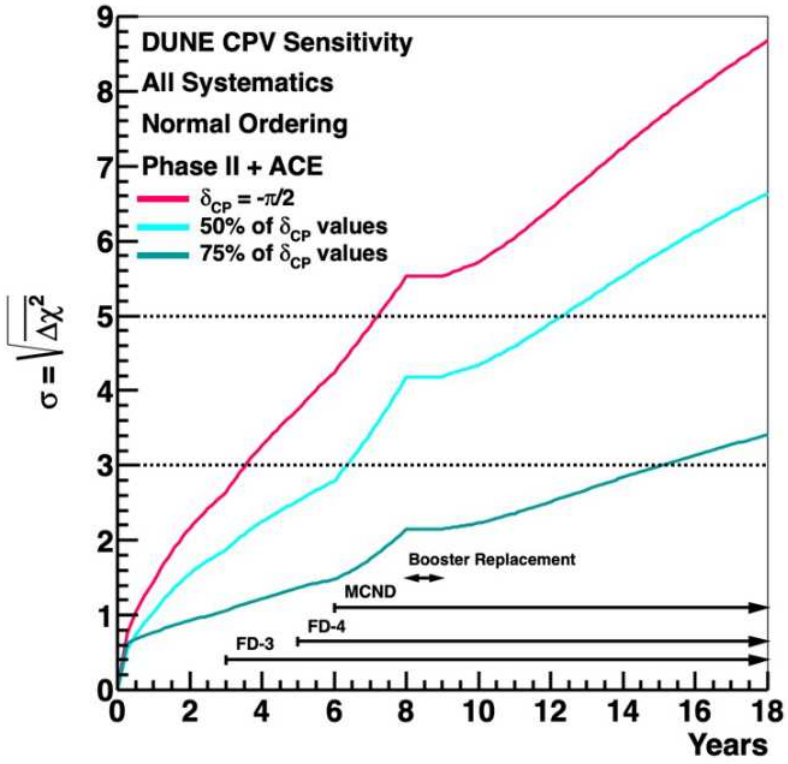

Figure 6. Sensitivity to $\delta_{CP} = -\pi/2$ and the coverage of δ_{CP} parameter space as a function of time at different significance levels assuming normal mass ordering from [41]. Horizontal arrows indicate progressive second-phase improvements such as further addition of two detector modules (FD-3, FD-4), the upgrade of near detector facility (MCND) for improvement of systematic uncertainties, or the beam power upgrade.

With largely different baselines of DUNE and Hyper-Kamiokande, there is great complimentarity between the two experiments with each measuring neutrino oscillation in distinct energy regions and being subject to different magnitudes of the matter effects. Ultimately, the combination of results from the two experiments can help shed light on a number of remaining unknowns in the mixing of massive neutrinos in addition to answering the question of whether CP violation exists in the lepton sector.

6. Conclusions

The breaking of the CP symmetry in nature is a fundamental requirement for the creation the matter-dominant universe and the search for sources of CP violation is pursued on many fronts. The discovery of neutrino oscillations and, by consequence, of the existence of the non-zero neutrino mass opened an additional door to explore CP violation in the lepton sector. While some positive hints of its existence might already be showing, they are yet to be confirmed as one enters the precision era in the studies of neutrino oscillations for the next two decades.

Funding: This research received no external funding.

Data Availability Statement: Data are contained within the article.

Conflicts of Interest: The author declares no conflict of interest.

Abbreviations

The following abbreviations are used in this manuscript:

BAU	Baryon Asymmetry of Universe
CP	Charge Parity
LBL	Long BaseLine
IO	Inverted Ordering
NO	Normal Ordering

References

1. Riotto, A.; Trodden, M. Recent progress in baryogenesis. *Ann. Rev. Nucl. Part. Sci.* **1999**, *49*, 35–75. [CrossRef]
2. Workman, R.L.; Burkert, V.D.; Crede, V.; Klempt, E.; Thoma, U.; Tiator, L.; Agashe, K.; Aielli, G.; Allanach, B.C.; Amsler, C.; et al. Review of Particle Physics. *Prog. Theor. Exp. Phys.* **2022**, *2022*, 083C01. [CrossRef]
3. Sakharov, A. Violation of CP invariance, C asymmetry, and baryon asymmetry of the universe. *J. Exp. Theor. Phys. Lett.* **1967**, *5*, 24–27.
4. Christenson, J.H.; Cronin, J.W.; Fitch, V.L.; Turlay, R. Evidence for the 2π Decay of the K_2^0 Meson. *Phys. Rev. Lett.* **1964**, *13*, 138–140. [CrossRef]
5. Jarlskog, C. Commutator of the Quark Mass Matrices in the Standard Electroweak Model and a Measure of Maximal CP Nonconservation. *Phys. Rev. Lett.* **1985**, *55*, 1039. [CrossRef] [PubMed]
6. Hou, W.S. Source of CP Violation for the Baryon Asymmetry of the Universe. *Chin. J. Phys.* **2009**, *47*, 134. [CrossRef]
7. Simkovic, F.; Bilenky, S.M.; Faessler, A.; Gutsche, T. Possibility of measuring the CP Majorana phases in $0\nu\beta\beta$ decay. *Phys. Rev. D* **2013**, *87*, 073002. [CrossRef]
8. Esteban, I.; Gonzalez-Garcia, M.C.; Maltoni, M.; Schwetz, T.; Zhou, A. The fate of hints: Updated global analysis of three-flavor neutrino oscillations. *J. High Energy Phys.* **2020**, *2020*, 178. [CrossRef]
9. Esteban, I.; Gonzalez-Garcia, M.C.; Maltoni, M.; Schwetz, T.; Zhou, A. NuFIT 5.2. 2022. Available online: www.nu-fit.org (accessed on 1 December 2023).
10. Aker, M.; Beglarian, A.; Behrens, J.; Berlev, A.; Besserer, U.; Bieringer, B.; Block, F.; Bobien, S.; Böttcher, M.; Bornschein, B.; et al. Direct neutrino-mass measurement with sub-electronvolt sensitivity. *Nat. Phys.* **2022**, *18*, 160–166. [CrossRef]
11. Aghanim, N.; Akrami, Y.; Ashdown, M.; Aumont, J.; Baccigalupi, C.; Ballardini, M.; Banday, A.J.; Barreiro, R.B.; Bartolo, N.; Basak, S.; et al. Planck 2018 results. VI. Cosmological parameters. *Astron. Astrophys.* **2020**, *641*, A6; Erratum: *Astron. Astrophys.* **2021**, *652*, C4. [CrossRef]
12. Yanagida, T. Horizontal gauge symmetry and masses of neutrinos. *Conf. Proc. C* **1979**, *7902131*, 95–99.
13. Buchmuller, W.; Peccei, R.D.; Yanagida, T. Leptogenesis as the origin of matter. *Ann. Rev. Nucl. Part. Sci.* **2005**, *55*, 311–355. [CrossRef]
14. Kopp, S.E. Accelerator-based neutrino beams. *Phys. Rept.* **2007**, *439*, 101–159. [CrossRef]
15. Freund, M. Analytic approximations for three neutrino oscillation parameters and probabilities in matter. *Phys. Rev. D* **2001**, *64*, 053003. [CrossRef]
16. Abe, K.; Adam, J.; Aihara, H.; Akiri, T.; Andreopoulos, C.; Aoki, S.; Ariga, A.; Ariga, T.; Assylbekov, S.; Autiero, D.; et al. Observation of Electron Neutrino Appearance in a Muon Neutrino Beam. *Phys. Rev. Lett.* **2014**, *112*, 061802. [CrossRef] [PubMed]
17. Adamson, P.; Ader, C.; Andrews, M.; Anfimov, N.; Anghel, I.; Arms, K.; Arrieta-Diaz, E.; Aurisano, A.; Ayres, D.S.; Backhouse, C.; et al. First measurement of electron neutrino appearance in NOvA. *Phys. Rev. Lett.* **2016**, *116*, 151806. [CrossRef]
18. Nunokawa, H.; Parke, S.; Valle, J.W. CP violation and neutrino oscillations. *Prog. Part. Nucl. Phys.* **2008**, *60*, 338–402. [CrossRef]
19. Apollonio, M.; Baldini, A.; Bemporad, C.; Caffau, E.; Cei, F.; Dèclais, Y.; de Kerret, H.; Dieterle, B.; Etenko, A.; Foresti, L.; et al. Search for neutrino oscillations on a long baseline at the CHOOZ nuclear power station. *Eur. Phys. J. C* **2003**, *27*, 331–374. [CrossRef]
20. Fukuda, Y.; Hayakawa, T.; Ichihara, E.; Inoue, K.; Ishihara, K.; Ishino, H.; Itow, Y.; Kajita, T.; Kameda, J.; Kasuga, S.; et al. Evidence for oscillation of atmospheric neutrinos. *Phys. Rev. Lett.* **1998**, *81*, 1562–1567. [CrossRef]
21. Guo, X.; Wang, N.; Wang, R.; Bishai, M.; Diwan, M.; Frank, J.; Hahn, R.L.; Li, K.; Littenberg, L.; Jaffe, D.; et al. A Precision Measurement of the Neutrino Mixing Angle θ_{13} Using Reactor Antineutrinos at Daya-Bay. *arXiv* **2006**, arXiv:1603.00278.
22. Ahn, J.K.; Baek, S.R.; Choi, S.; Choi, Y.; Chung, I.S.; Danilov, N.; Jang, J.S.; Jeon, E.J.; Joo, K.K.; Jung, Y.H.; et al. RENO: An Experiment for Neutrino Oscillation Parameter θ_{13} Using Reactor Neutrinos at Yonggwang. *arXiv* **2010**, arXiv:1003.1391.
23. Ardellier, F.; Barabanov, I.; Barriere, J.C.; Beiel, F.; Berridge, S.; Bezrukov, L.B.; Bernstein, A.; Bolton, T.; Bowden, N.S.; Buck, C.; et al. Double Chooz: A Search for the neutrino mixing angle theta(13). *arXiv* **2006**, arXiv:hep-ex/0606025.

24. Letter of Intent: Neutrino Oscillation Experiment at JHF. 2003. Available online: https://neutrino.kek.jp/jhfnu/loi/loi.v2.030528.pdf (accessed on 1 December 2023)
25. Beavis, D.; Carroll, A.; Chiang, I.; Diwan, M.; Frank, J.; Khan, S.; Marx, M.; McCorkle, S.; Murtagh, M.; Sondericker, J.; et al. *Long Baseline Neutrino Oscillation Experiment at the AGS Approved by the HENPAC as AGS Experiment 889*; INSPIRE-HEP: Cedar City, UT, USA, 1995. [CrossRef]
26. Ayres, D.S.; Dawson, J.W.; Drake, G.; Goodman, M.C.; Grudzinski, J.J.; Guarino, V.J.; Joffe-Minor, T.; Reyna, D.E.; Talaga, R.L.; Thron, J.L.; et al. NOvA: Proposal to Build a 30 Kiloton Off-Axis Detector to Study $\nu_\mu \rightarrow \nu_e$ Oscillations in the NuMI Beamline. *arXiv* **2004**, arXiv:0503053.
27. Long, K. Neutrino factory R&D. *Nucl. Phys. B Proc. Suppl.* **2006**, *154*, 111–122. [CrossRef]
28. Long, K. The neutrino factory: Physics and accelerator concepts. *Acta Phys. Pol. B* **2006**, *37*, 2059–2075.
29. Zucchelli, P. A novel concept for a $\overline{\nu}_e/\nu_e$ neutrino factory: The beta beam. *Phys. Lett. B* **2002**, *532*, 166–172. [CrossRef]
30. Abe, K.; Abgrall, N.; Ajima, Y.; Aihara, H.; Albert, J.B.; Andreopoulos, C.; Andrieu, B.; Aoki, S.; Araoka, O.; Argyriades, J.; et al. Indication of Electron Neutrino Appearance from an Accelerator-produced Off-axis Muon Neutrino Beam. *Phys. Rev. Lett.* **2011**, *107*, 041801. [CrossRef]
31. An, F.P.; Bai, J.Z.; Balantekin, A.B.; Band, H.R.; Beavis, D.; Beriguete, W.; Bishai, M.; Blyth, S.; Boddy, K.; Brown, R.L.; et al. Observation of electron-antineutrino disappearance at Daya Bay. *Phys. Rev. Lett.* **2012**, *108*, 171803. [CrossRef]
32. An, F.P.; Bai, W. D.; Balantekin, A.B.; Bishai, M.; Blyth, S.; Cao, G.F.; Cao, J.; Chang, J.F.; Chang, Y.; Chen, H.S.; et al. Precision Measurement of Reactor Antineutrino Oscillation at Kilometer-Scale Baselines by Daya Bay. *Phys. Rev. Lett.* **2023**, *130*, 161802. [CrossRef]
33. Abe, K.; Akutsu, R.; Ali, A.; Alt, C.; Andreopoulos, C.; Anthony, L.; Antonova, M.; Aoki, S.; Ariga, A.; Arihara, T.; et al. Constraint on the matter–antimatter symmetry-violating phase in neutrino oscillations. *Nature* **2020**, *580*, 339–344; Erratum: *Nature* **2020**, *583*, E16. [CrossRef]
34. Abe, K.; Akhlaq, N.; Akutsu, R.; Ali, A.; Alonso Monsalve, S.; Alt, C.; Andreopoulos, C.; Antonova, M.; Aoki, S.; Arihara, T.; et al. Measurements of neutrino oscillation parameters from the T2K experiment using 3.6×10^{21} protons on target. *Eur. Phys. J. C* **2023**, *83*, 782. [CrossRef] [PubMed]
35. Acero, M.A.; Adamson, P.; Aliaga, L.; Anfimov, N.; Antoshkin, A.; Arrieta-Diaz, E.; Asquith, L.; Aurisano, A.; Back, A.; Backhouse, C.; et al. Improved measurement of neutrino oscillation parameters by the NOvA experiment. *Phys. Rev. D* **2022**, *106*, 032004. [CrossRef]
36. Abe, K.; Bronner, C.; Haga, Y.; Hayato, Y.; Ikeda, M.; Iyogi, K.; Kameda, J.; Kato, Y.; Kishimoto, Y.; Marti, L.; et al. Atmospheric neutrino oscillation analysis with external constraints in Super-Kamiokande I-IV. *Phys. Rev. D* **2018**, *97*, 072001. [CrossRef]
37. Abe, K.; Abe, K.; Aihara, H.; Aimi, A.; Akutsu, R.; Andreopoulos, C.; Anghel, I.; Anthony, L.H.V.; Antonova, M.; Ashida, Y.; et al. Hyper-Kamiokande Design Report. *arXiv* **2018**, arXiv:1805.04163.
38. Abi, B.; Acciarri, R.; Acero, M.A.; Adamov, G.; Adams, D.; Adinolfi, M.; Ahmad, Z.; Ahmed, J.; Alion, T.; Alonso Monsalve, S.; et al. Deep Underground Neutrino Experiment (DUNE), Far Detector Technical Design Report, Volume I Introduction to DUNE. *J. Instrum.* **2020**, *15*, T08008. [CrossRef]
39. Scott, M. Long-baseline neutrino oscillation sensitivities with Hyper-Kamiokande. *PoS* **2021**, *390*, 174. [CrossRef]
40. Bishai, M. P5 Townhall Meeting, DUNE Far Detectors—Phase II. 2023. Available online: https://indico.fnal.gov/event/58272/contributions/262191/ (accessed on 1 December 2023).
41. Marshall, C. P5 Townhall Meeting, DUNE Far Detectors—Phase II. 2023. Available online: https://indico.fnal.gov/event/58272/contributions/262187/ (accessed on 21 March 2023).